

# Endothelial cells are a replicative niche for entry of *Toxoplasma gondii* to the central nervous system

Christoph Konradt<sup>1</sup>, Norikiyo Ueno<sup>2</sup>, David A. Christian<sup>1</sup>, Jonathan H. Delong<sup>1</sup>,  
Gretchen Harms Pritchard<sup>1</sup>, Jasmin Herz<sup>3</sup>, David J. Bzik<sup>4</sup>, Anita A. Koshy<sup>5</sup>, Dorian B. McGavern<sup>3</sup>,  
Melissa B. Lodoen<sup>2</sup> and Christopher A. Hunter<sup>1\*</sup>

An important function of the blood-brain barrier is to exclude pathogens from the central nervous system, but some microorganisms benefit from the ability to enter this site. It has been proposed that *Toxoplasma gondii* can cross biological barriers as a motile extracellular form that uses transcellular or paracellular migration, or by infecting a host cell that then crosses the blood-brain barrier. Unexpectedly, analysis of acutely infected mice revealed significant numbers of free parasites in the blood and the presence of infected endothelial cells in the brain vasculature. The use of diverse transgenic parasites combined with reporter mice and intravital imaging demonstrated that replication in and lysis of endothelial cells precedes invasion of the central nervous system, and highlight a novel mechanism for parasite entry to the central nervous system.

**R**eactivation of latent *Toxoplasma gondii* infection in the brain causes significant disease in immune deficient individuals<sup>1</sup>. Several major mechanisms have been proposed to explain how pathogens, including *T. gondii*, access the brain<sup>2–6</sup>. In one scenario, the ability of microorganisms in the blood to perform para- or transcellular migration<sup>7–10</sup> may allow them to cross the blood-brain barrier (BBB). Alternatively, the ‘Trojan horse’ hypothesis suggests that the ability of infected cells to disseminate from sites of infection can promote pathogen spread into the brain<sup>3,6,11–13</sup>. Toxoplasmosis in mice provides a natural model system to study host-pathogen interactions, and advances in live imaging have provided new insights into the immune response to *T. gondii*<sup>14</sup>. Indeed, multi-photon (MP) microscopy using Tie2-GFP mice to visualize endothelial cells (ECs) and fluorescent parasites has been combined with a variety of transgenic parasite strains and transfer systems to characterize host-pathogen interactions in the meningeal and parenchymal compartments of the neocortex<sup>15–17</sup>.

## Results

***T. gondii* infection of the vascular compartment.** To study *T. gondii* in the vascular compartment, Tie2-GFP reporter mice were infected intraperitoneally (i.p.) with tachyzoites (Fig. 1a,b,e) or orally with cysts (Fig. 1c,d,f–g) using a *T. gondii* strain expressing the tdTomato fluorescent protein (Pru-tdTomato). By 7 days post infection (d.p.i.), infected neocortical ECs were observed, regardless of the route of infection (Fig. 1a,b,d–e, Supplementary Fig. 1a,f). The appearance of multiple organisms within a single parasitophorous vacuole (PV) and green fluorescent protein (GFP) displacement indicates the presence of replicating parasites within the ECs (Fig. 1b,d,e). This observation was unexpected, as ECs have not been described as a major target of *T. gondii* *in vivo*. By 8 d.p.i., the foci of parasite replication were located in the parenchyma of the neocortex, but were still closely

associated with ECs lining the blood vessel (Fig. 1c and Supplementary Fig. 1b,c). By 15 d.p.i., a time point when the cyst form of the parasite starts to appear in the central nervous system (CNS), these latent developmental stages could be identified based on size and morphology and were observed within the neocortex parenchyma in close proximity to blood vessels (Supplementary Fig. 1e). Flow cytometry was used to identify ECs based on their expression of CD31 and CD102 and the absence of CD45<sup>18</sup> and at 8 days post oral (Fig. 1f,g) or i.p. (Supplementary Fig. 2) infection, Pru-tdTomato was detected in ~1.5% of lung ECs and 0.01% of brain ECs (Fig. 1f,g). A normal mouse brain harbours approximately 7 million vessel-related ECs<sup>19</sup>, so it appears that less than 1,000 brain ECs were infected at this early time point. These approaches establish that during acute toxoplasmosis there is a transient population of infected ECs that precedes dissemination into the CNS and presumably other tissues.

Previous reports have described monocytes infected with *T. gondii* in the blood during acute infection, and it has been proposed that these cells transport parasites across the BBB<sup>6</sup>. In our experiments, at similar time points, infected cells present in the blood expressed a variety of surface markers (CD11b, CD3, Gr1 and CD11c) associated with monocytes, T cells, neutrophils and dendritic cells (DCs) (Supplementary Fig. 3). Similar to previous studies<sup>6</sup>, the intravenous (i.v.) transfer of monocytes infected with a replication-deficient strain of *T. gondii* (CPS)<sup>20</sup> into naive or infected mice allowed the detection of infected cells in the whole brain at 24 and 48 h post transfer. The invasion of host cells by the CPS strain is associated with normal secretion of parasite effectors<sup>20,21</sup>, and infected monocytes displayed hyper-dissemination from sites of infection, as has been reported previously<sup>22</sup>. However, the i.v. injection of an antibody to the cell surface marker CD45 allowed us to distinguish vascular and extravascular populations of infected cells, and revealed that these cells were exclusively resident in the vascular compartment (Supplementary Fig. 6).

<sup>1</sup>Department of Pathobiology, School of Veterinary Medicine, University of Pennsylvania, Philadelphia, Pennsylvania, 19104, USA. <sup>2</sup>Department of Molecular Biology and Biochemistry and Institute for Immunology, University of California, Irvine, California, 92697, USA. <sup>3</sup>National Institute of Neurological Disorders and Stroke, The National Institutes of Health, Bethesda, Maryland, 20892, USA. <sup>4</sup>Department of Microbiology and Immunology, Geisel School of Medicine at Dartmouth, Lebanon, New Hampshire, 03756, USA. <sup>5</sup>Department of Neurology, University of Arizona, Tucson, Arizona, 85724, USA.

\*e-mail: chunter@vet.upenn.edu

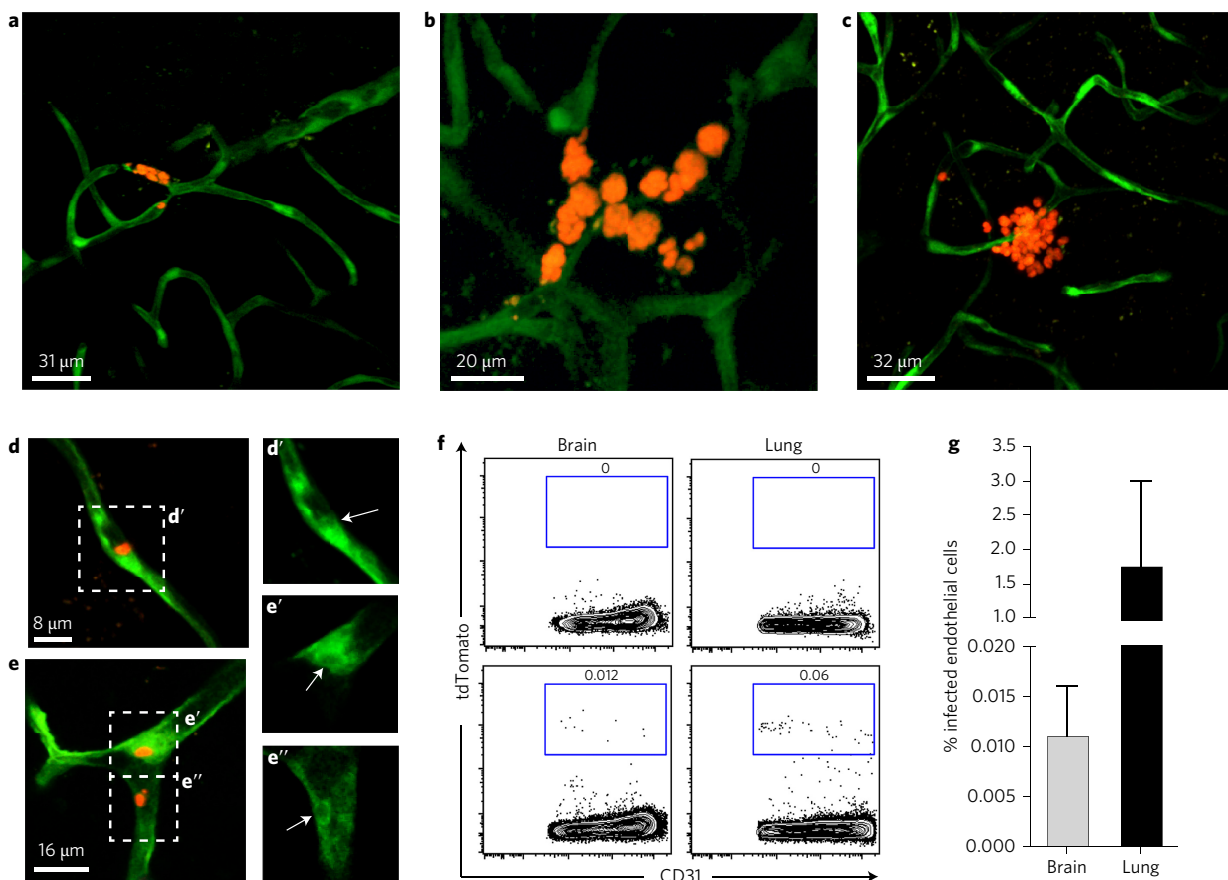


**Figure 1 |** *T. gondii* infection of the vascular compartment. **a-c**, Representative maximum projections of multiphoton stacks of brain slices showing Tie2-GFP reporter mice at 7 d.p.i. (**a,b**) or 8 d.p.i. (**c**). **d,e**, Brain slices at 7 d.p.i. showing *T. gondii* parasites (red) within ECs (green). **d',e',e''**, Confocal planes through the infected ECs. White arrows indicate GFP displacement. Images shown are representative of three independent experiments ( $n = 5$  mice per experiment). **f,g**, Detection and quantification of infected endothelial cells at day 8 post oral infection using flow cytometry to detect infected lung and brain CD31+ and CD102+ endothelial cells. % infected ECs are the mean  $\pm$  s.e.m.; data are from three independent experiments ( $n = 5$  mice per experiment).

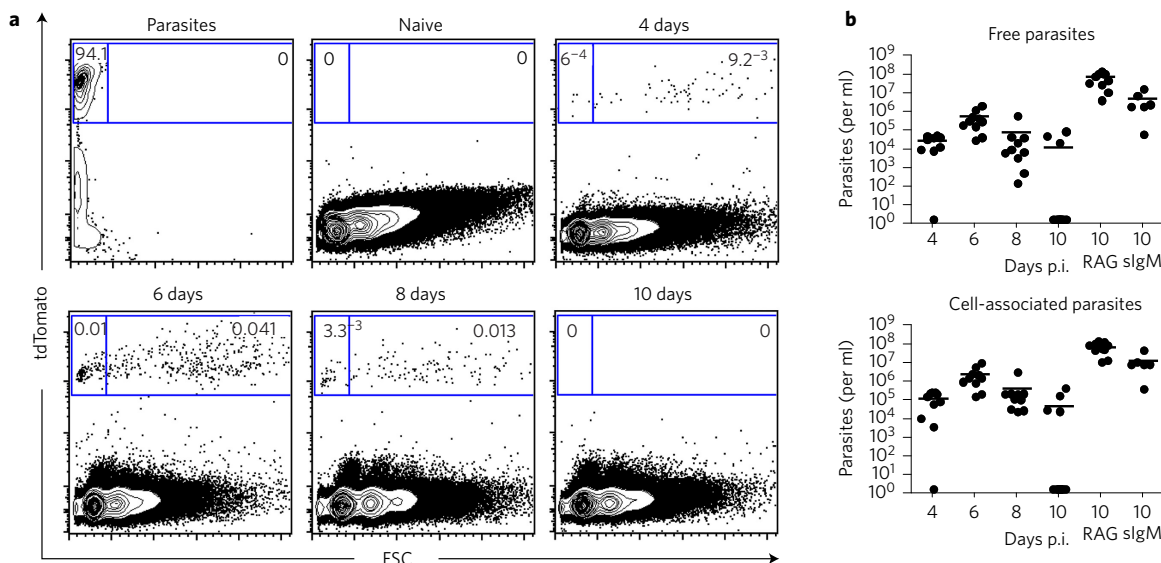


**Figure 2 |** Detection of free *T. gondii* tachyzoites in the vascular compartment. C57BL/6 mice were infected with  $1 \times 10^5$  *T. gondii* tachyzoites expressing tdTomato, and the blood was analysed by flow cytometry. **a**, Representative flow cytometry plots of tdTomato versus forward scatter (FSC) as a measure of cell size show the ability to distinguish free parasites from infected cells. Parasites isolated from tissue culture are shown in the first panel and have a low FSC and are detected in a tight left gate. Cell associated parasites have a high FSC and are present in a broader right gate. They can be detected in infected mice starting at day 4 post infection, but are absent by day 10. **b**, Kinetics and quantification of free and cell-associated parasites in the blood. Lymphocyte-deficient (RAG) mice and secretory IgM-KO (slgM) mice are unable to control the parasite burden. Data are from three independent experiments and each dot represents a single mouse ( $n = 20$  mice per experiment).

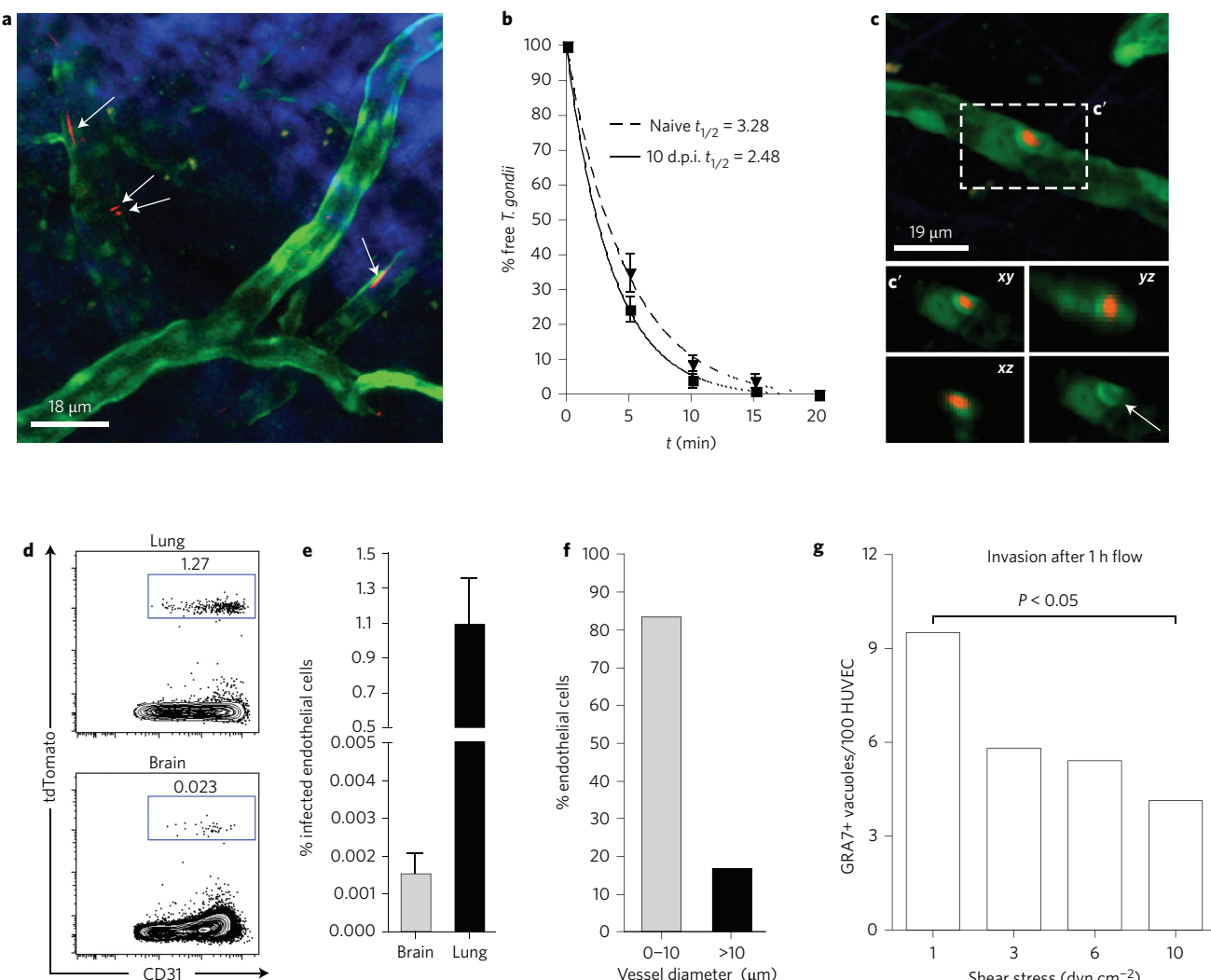


**Figure 3 |** *T. gondii* tachyzoites invade ECs *in vivo* and *in vitro*. Tie2-GFP reporter mice were infected i.v. with  $1 \times 10^7$  to  $2 \times 10^7$  tachyzoites that express tdTomato. **a**, Free parasites (white arrows) are seen in the vascular compartment 1 minute after injection. **b**, The numbers of parasites per imaging field in **a** were counted over time to calculate the half life ( $t_{1/2}$ ) of free parasites present in the circulation in naive mice ( $n = 10$ ) or in mice 10 days post oral infection ( $n = 5$ ). **c**, Representative maximum projection of *T. gondii* (red) infected ECs (green) 1 h after i.v. challenge. **c'**, Single planes through an infected EC. The white arrow indicating GFP displacement. Images are representative of three independent experiments using individual mice. **d**, Representative flow cytometry plots of C57BL/6 mice infected i.v. with tdTomato-expressing tachyzoites. CD102+ and CD31+ endothelial cells isolated 1 h.p.i. **e**, Quantification of the number of infected ECs (mean  $\pm$  s.e.m., data are pooled from three independent experiments,  $n = 5$  mice per experiment). **f**, Over 80% of the tachyzoites interacted with ECs in vessels with a diameter smaller than 10  $\mu\text{m}$  at 7–9 d.p.i. ( $n = 30$  vessels counted in 12 infected mice). **g**, Infection frequency of HUVEC monolayers in a microfluidic chamber under different shear stress conditions. Bars represent mean  $\pm$  s.e.m. from two (1 and 6  $\text{dyn cm}^{-2}$ ) or three (3 and 10  $\text{dyn cm}^{-2}$ ) independent experiments.  $P < 0.05$ , two-tailed Student's *t*-test, comparing 1 and 10  $\text{dyn cm}^{-2}$ . A total of 1,717 PVs were scored.

**Detection of free *T. gondii* tachyzoites in the vascular compartment.** The data from the previous section indicate that infected monocytes do not readily cross the BBB, but the detection of infected ECs suggested that parasites can invade ECs from the vascular compartment, directly as free parasites or following egress from infected mononuclear cells. Indeed, when whole blood from mice infected orally or i.p. was analysed by flow cytometry, a significant population of free tachyzoites was detected (Fig. 2a and Supplementary Fig. 4), which correlated with the initial infectious dose (Supplementary Fig. 4a–e). Following a challenge dose of  $1 \times 10^5$  parasites i.p. (Fig. 2b), free parasites were first detected in the blood at 4 d.p.i., peaked at 6 d.p.i., and by 10 d.p.i. 70% of the mice were negative for parasites in this compartment. It is notable that mice deficient in B and T cells or IgM secretion maintained high levels of free parasites in the blood (Fig. 2b). Because parasite-induced IgM titres

start to increase by day 7 post infection<sup>23</sup>, these data indicate a key role for parasite-specific IgM in the control of *T. gondii* parasitaemia.

To calculate the length of time that free *T. gondii* tachyzoites circulate in the blood, naive or orally infected Tie2-GFP reporter mice were injected i.v. with  $1 \times 10^7$  to  $2 \times 10^7$  parasites expressing tdTomato (RH-tdTomato) and imaged. Parasites were observed passing through the vasculature (Fig. 3a and Supplementary Video 1) for  $\sim 10$ –15 min, but by 30 min parasites were rarely detected. Based on the change in number of tachyzoites passing through the field of view per minute, the mean circulation half-lives of the parasites in naive and infected mice were estimated to be  $3.28 \pm 0.27$  (s.e.m.) min and  $2.48 \pm 0.21$  min, respectively (Fig. 3b,  $P = 0.8955$ ). This short half-life, combined with the number of free parasites in the blood, indicates that there is a considerable transient burden of extracellular parasites in the blood during acute infection.

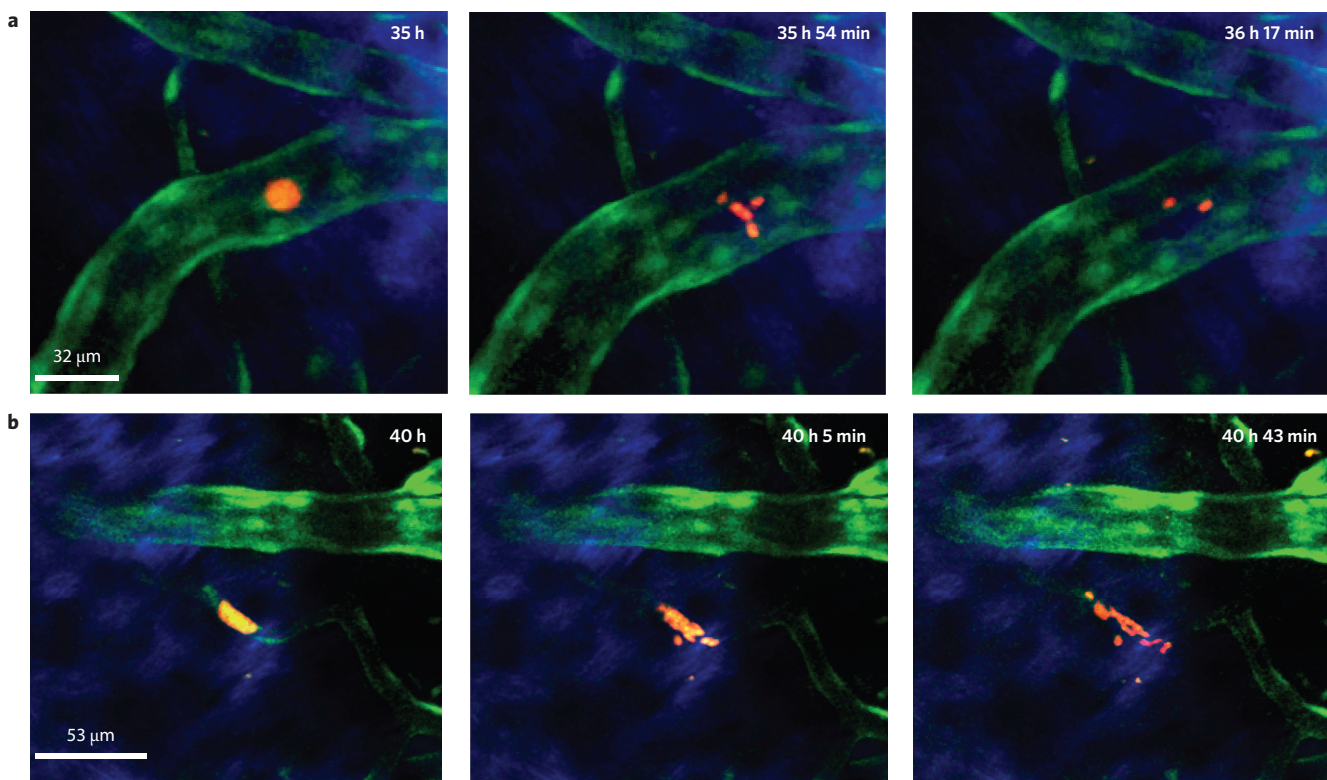


**Figure 4 | *T. gondii* egress from ECs *in vivo*.** **a,b,** Intravital multiphoton imaging through a thinned skull window of a Tie2-GFP reporter mouse infected i.v. with tdTomato-expressing tachyzoites, showing image sequences of the egress of *T. gondii* (red) out of an infected EC (green). Images provided are from individual mice, and egress was observed five times.

***T. gondii* tachyzoites invade ECs *in vivo* and *in vitro*.** To determine whether free tachyzoites in the blood could directly invade ECs *in vivo*, Tie2-GFP reporter mice were injected i.v. with  $1 \times 10^7$  to  $2 \times 10^7$  RH-tdTomato tachyzoites and brain explants were surveyed using MP microscopy. Within minutes after injection, infected brain ECs could be detected (Fig. 3c). The use of flow cytometry revealed that 1 h after i.v. infection, 0.015% and 1.1% of the ECs in the brain and lung, respectively, were infected (Fig. 3d,e) and the parasites were preferentially associated with the CD31hi population. Thus, free parasites present in the vascular compartment are readily able to invade ECs in different tissues.

One feature that was apparent in the brain, regardless of the route of infection, was that many of the infected ECs were present in smaller blood vessels, and quantification revealed that over 80% of the infected ECs were in vessels with a diameter of less than  $10 \mu\text{m}$  (Fig. 3f). Because blood flow rates and shear stress levels differ in vessels of different sizes<sup>24</sup>, experiments were performed to investigate whether the flow rate had an impact on EC invasion. In these studies, tachyzoites were flowed over a monolayer of primary human umbilical vein endothelial cells (HUVECs) in a microfluidic chamber under different shear force conditions that reflect those reported *in vivo*<sup>25,26</sup>. Cells were then stained with antibodies against the dense granule protein GRA7 to identify intracellular parasites. These experiments demonstrated that the invasion rate decreased with increasing shear force conditions (Fig. 3g). These results are consistent with previous work that implicated differential flow rates as a key determinant of the ability of *Neisseria meningitidis* to adhere to ECs in cerebral capillaries<sup>27</sup>, and may explain the preferential localization of *T. gondii* within cerebral capillaries.

To understand the fate of infected ECs, Tie2-GFP reporter mice were infected i.v. with RH-tdTomato, and were prepared for imaging 2 days later. The i.v. introduction of microorganisms has been useful to understand how pathogens disseminate from the blood<sup>10,13,28–31</sup>, and this approach maximized the opportunity to

visualize the fate of infected cells. At this time point, multiple parasites were observed within a single PV in vessels within the meninges and neocortex (Fig. 4a,b), and between 30 and 45 h post infection (h.p.i.), parasite egress could be observed. In Fig. 4a and Supplementary Video 2, most tachyzoites have exited into the blood vessel lumen, but two tachyzoites remain localized in neighbouring cells (Supplementary Fig. 5b–d). In Fig. 4b and Supplementary Video 3, following lysis of the infected ECs in a small blood vessel, all parasites remained in close proximity. The loss of the GFP signal after parasite egress indicates EC lysis (Supplementary Videos 3 and 4). Additional imaging of areas of parasite-mediated EC lysis did not reveal recruitment of platelets or neutrophils or overt signs of haemorrhage. These studies, together with the images presented in Fig. 1, indicate that parasite replication and EC lysis is associated with the development of local foci of replication and dissemination into the CNS.

**Replication of *T. gondii* in ECs is required for parasites to cross the BBB.** Although our studies demonstrate the unexpected presence of free parasites in the vascular compartment and the lysis of infected ECs, it was unclear whether these latter events were required for *T. gondii* to cross the BBB. To address whether extracellular parasites can directly access the parenchyma from the blood, mice were injected i.v. with the non-replicating type I *T. gondii* strain (CPS-mCherry) or the parental replication competent wild-type (WT) strain (RH-tdTomato). To distinguish the two fluorescent strains, the CPS strain was also labelled with violet cell trace (VCT)<sup>21</sup>. A 1:1 mixture of these strains was used to infect the Tie2-GFP mice i.v., and at 1 h.p.i., the two strains infected a similar frequency of ECs in the brain and lung (Fig. 5a). By 48 h.p.i., the replication of the parental strain resulted in a 30-fold change in the ratio of infected brain ECs between CPS and RH (where RH is the strain used)

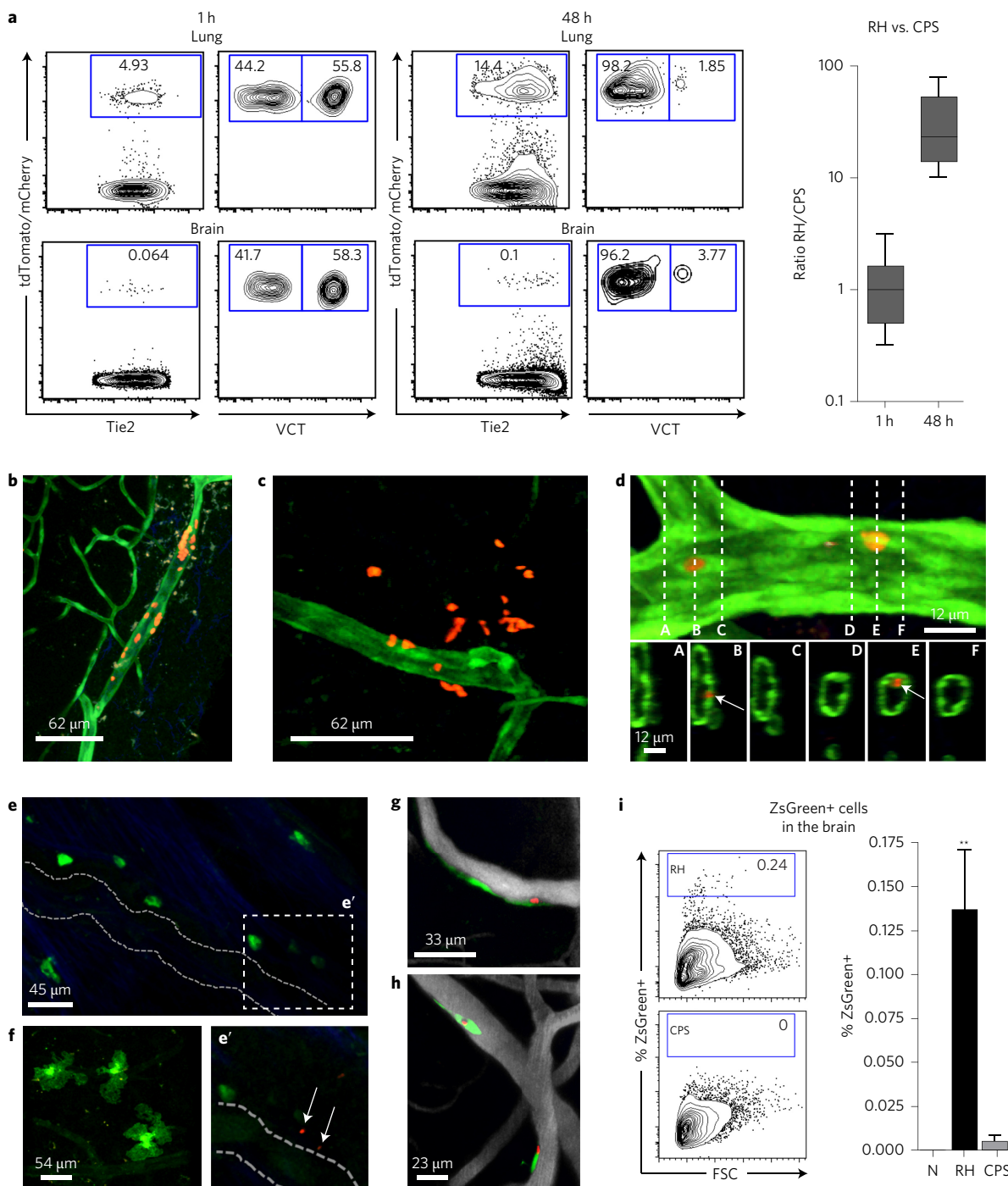


**Figure 5 |** Replication of *T. gondii* in ECs is required for parasites to cross the BBB. **a**, Representative flow cytometry plots of a competition assay between RH-tdTomato and CPS-mCherry. The CPS strain was labelled with VCT to distinguish the two strains, and Tie2-GFP mice were infected i.v. with a 1:1 ratio of parasites. ECs in the lung and brain were analysed after 1 h and 48 h, and the ratio of RH:CPS in the brain was calculated at these time points. The histogram shows mean  $\pm$  s.e.m., and data are pooled from three independent experiments ( $n = 3$  mice per time point and experiment). **b-d**, Representative maximum projections of multiphoton stacks 48 h.p.i. of brain slices from six Tie2-GFP reporter mice i.v. infected with RH-tdTomato (**b,c**) or CPS-mCherry (**d**) tachyzoites. Lower panels in **d** show single y-z planes of the line cuts shown in the main panel. White arrows indicate two parasites. **e-h**, Ai6 reporter mice were infected i.v. with RH-Cre-mCherry (**e,f**) or CPS-Cre-mCherry (**g,h**) tachyzoites and assessed at 24 h (**g**) and 48 h (**e,f,h**) post infection. Dotted lines in **e** indicate the blood vessel border (enlarged view shown in **e'**). Images shown are representative of three independent experiments ( $n = 2$  mice per condition and experiment). **i**, Analysis of mononuclear brain cells at 72 h.p.i. reveals the appearance of ZsGreen<sup>+</sup> cells in the brain parenchyma in mice infected with the WT strain but not with the CPS mutant. Note that this analysis specifically excludes CD102<sup>+</sup> endothelial cells (mean  $\pm$  s.e.m.; data are from two independent experiments,  $n = 5$  and 4 mice,  $^{**}P < 0.0017$ , two-tailed Student's *t*-test).

(Fig. 5a,  $P < 0.0017$ ). MP microscopy confirmed the high frequency of ECs infected with RH in the vasculature of the neocortex at this time (Fig. 5b), and tachyzoites were detected within the brain

parenchyma of mice infected with the replication sufficient parental strain (Fig. 5c). However, in mice infected with CPS-mCherry, single parasites could be detected within ECs (Fig. 5d)

but not in the parenchyma, indicating that these organisms are unable to undergo a para- or trans-cellular transmigration across the BBB.

Because it was possible that the CPS-mCherry parasites cross the BBB but are cleared, parasites that secrete Cre recombinase with their rhoptry effector proteins were combined with transgenic mice (Ai6), in which the ZsGreen fluorescent reporter protein is under the control of a promoter that contains a floxed STOP codon. This system allows the identification of cells that had been injected with parasite proteins during invasion<sup>32</sup>. Infection with the RH-Cre strain i.v. resulted in the detection of ZsGreen+ cells beyond the vessel wall (white dotted line in Fig. 5e) and in the parenchyma of the neocortex at 48 h.p.i. (Fig. 5e,f). In contrast, non-replicating CPS-Cre parasites were able to induce ZsGreen expression in the brain, but the location and morphology of these cells identified them as ECs (Fig. 5g,h). The lack of spread into the parenchyma by the CPS parasite was not due to parasite death, as infected ECs were detected at 24 h.p.i. (Fig. 5g) and 48 h.p.i. (Fig. 5h), but these results do not rule out the possibility that nutrient stress of these mutants might affect the events required for egress and invasion of new host cells. Furthermore, fluorescence-activated cell sorting (FACS) analysis of mononuclear cell preparations prepared from the brain at 72 h.p.i., which excluded the EC populations, confirmed the presence of ZsGreen+ cells in mice infected with the WT strain but not with the CPS-Cre mutant (Fig. 5i). These data establish that tachyzoites of *T. gondii* do not readily translocate into the brain, and replication within and lysis of ECs precedes parasites crossing the BBB.

## Discussion

The availability of transgenic and replication-deficient parasites combined with reporter mice and intravital imaging has allowed us to visualize and characterize the interactions of *T. gondii* with ECs. Although there is evidence that the 'Trojan horse' mechanism has a role in the dissemination of *T. gondii* from local sites of infection<sup>4,33,34</sup>, we were unable to show that infected cells crossed the BBB in naive or infected mice. Rather, the natural host-pathogen system utilized here provides an alternative explanation for how *T. gondii* invades the CNS, and demonstrates the presence of free parasites in the blood and that this organism compromises the BBB by invading, replicating in, and lysing ECs. There are still many basic questions about the processes used by neurotropic pathogens to access the CNS, and this mechanism may be relevant to other viral, bacterial parasitic and fungal organisms that disseminate through the blood and can infect ECs *in vitro*<sup>3,14,15,35</sup>. For *T. gondii*, the finding that IgM is required to resolve the parasitaemia suggests that prophylactic antibody treatment may prove useful to specifically limit the ability of extracellular parasites in the blood to disseminate to the brain as well as other clinically relevant sites such as the placenta and eye.

Our studies also highlight new questions about the interactions between ECs and *T. gondii* that are relevant to the pathogenesis of this disease. There are other pathogens, such as the Nipah virus, that replicate extensively in ECs and are associated with haemorrhagic disease<sup>36</sup>. However, our preliminary studies indicate that *T. gondii*-mediated EC lysis was not associated with local haemorrhages, perhaps because this is a relatively isolated event, or because *T. gondii* may have evolved mechanisms of parasite egress that limit bystander damage. Nevertheless, there is a significant parasite burden in the blood, and additional studies are needed to understand its impact on inflammation in the vascular compartment and whether ECs can be activated *in vivo* to control parasite replication. The other major question relates to the preferential localization of *T. gondii* in cerebral microvessels and whether there is a tropism for capillary or post-capillary venules, and if the lower blood flow rate and/or increased surface area in capillaries

explains parasite localization. It is known that, *in vivo*, in vessels with low shear stresses, particularly at bifurcations, there are unstable flow conditions that include 'stagnant' blood areas<sup>27</sup>. These types of event may provide sufficiently low velocities to allow free tachyzoites of *T. gondii* the opportunity to adhere to and invade ECs.

For *T. gondii*, and other apicomplexans including Neospora and Hammondia, the development of cysts in tissues distal from initial sites of infection is a key factor in the transmission of these organisms<sup>37</sup>. Consequently, the ability to cross EC barriers is essential for parasite success, and the ability of *T. gondii* to infect and lyse ECs provides an unanticipated mechanism to overcome this bottleneck. For other vector-borne apicomplexans, the relationship with ECs is different: some avian and reptilian Plasmodium species initially replicate within ECs, while in *Plasmodium falciparum* and *Babesia* species the ability of infected erythrocytes to adhere to ECs allows parasite sequestration to avoid clearance and promote transmission<sup>38</sup>. The varied interactions of apicomplexan parasites with ECs reflect the different strategies used by these organisms to evade the immune system and to facilitate transmission, highlighting the importance of pathogen-EC interactions for microorganisms present, even transiently, in the vascular compartment.

## Methods

**Mice and infections.** Seven- to eight-week-old female C57BL/6 mice were obtained from Taconic Farms. Tie2-GFP, Ai6 and RAG mice were obtained from the Jackson Laboratories and were bred in the University Laboratory Animal Resources facilities at the University of Pennsylvania and used at seven to ten weeks of age for experiments. All procedures were performed in accordance with the guidelines of the University of Pennsylvania Institutional Animal Care and Use Committee.

RH-OVA-tdTomato and Pru-OVA-tdTomato parasites were grown in human foreskin fibroblast (HFF) monolayers cultured with D10 media (DMEM, 25% M199 supplement, 10% fetal bovine serum, 0.5% penicillin/streptomycin (10,000 mg/ml), 0.5% gentamycin (50 mg/ml)) as described previously<sup>39</sup>. The HFFs were purchased from the ATCC; they were not authenticated in this laboratory but were periodically tested for mycoplasma contamination using an antigen detection enzyme-linked immunosorbent assay. RH-Cre-mCherry and CPS-Cre-mCherry parasites were obtained from J. Boothroyd and A. Koshy and passaged as described in ref. 40. Mice were infected either i.p. with  $1 \times 10^4$ ,  $1 \times 10^5$  or  $1 \times 10^6$  tachyzoites in 100  $\mu$ l PBS, i.v. with  $1 \times 10^7$  to  $2 \times 10^7$  tachyzoites in 50  $\mu$ l PBS, or orally with 300 cysts in 0.2 ml PBS. For the competition assays the RH or CPS strain of *T. gondii* were stained with CellTrace Violet (Life Technologies).

**Experimental design and statistical approaches.** In individual experiments, mice of the same sex, age and strain were used to avoid bias, and there was no randomization or blinding of experimental groups. The sample size utilized was determined based on individual experiments, and for the imaging experiments individual mice were considered biological replicates. In the studies to quantify the numbers of infected ECs, groups of three to five mice were used, and individual mice were considered technical replicates. No mice were excluded from analysis. For experiments where we expected a variability representing <40% of the mean for each group, five mice per group were used to exceed a confidence interval of 95%. Statistical significance was determined using a Student's *t*-test.

**MP microscopy.** Mice were anaesthetized and maintained at a core temperature of 37 °C. Thinned-skull and open-skull surgery were performed as described previously<sup>41</sup>. For *ex vivo* imaging, mice were euthanized by CO<sub>2</sub> asphyxiation, and the brains were removed immediately with minimal mechanical disruption and placed in a heated chamber where specimens were constantly perfused with warmed (37 °C), oxygenated medium (phenol-red free RPMI 1640 supplemented with 10% FBS, Gibco). The temperature in the imaging chamber was maintained at 37 °C using heating elements, and was monitored using a temperature-control probe (Fine Science Tools). Imaging was performed with a Leica SP5 two-photon microscope system (Leica Microsystems) equipped with a picosecond or femtosecond laser (Coherent). The standard wavelength used for the two-photon imaging was 900 nm, which allowed optimal excitation of the used fluorophores, except mCherry, expressed by the RH-Cre strain. Therefore, acquiring the same image with wavelengths of 900 and 820 nm helped to identify ZsGreen positive cells as well as parasites in the parenchyma. Images were obtained using a  $\times 20$  water-dipping lens. The resulting images were analysed with Velocity software (PerkinElmer).

**Isolation of lung and brain cell preparations.** Mice were euthanized by CO<sub>2</sub> asphyxiation and then perfused with 20 ml cold PBS and 20 ml RPMI medium containing 1 mg ml<sup>-1</sup> collagenase A and 200  $\mu$ g DNase. Lungs were additionally

lavaged with RPMI medium containing 1 mg ml<sup>-1</sup> collagenase A and 200 µg DNase. After removal, the brain was homogenized by syringe passages through 18-, 22- and 26-gauge needles, then digested in 5 ml RPMI medium containing 1 mg ml<sup>-1</sup> collagenase A and 200 µg ml<sup>-1</sup> DNase for 1 h at 37 °C. The cell suspension was then washed and fractionated on a 25–50% percoll gradient (Pharmacia) for 20 min. The cells at the interface consisted of brain ECs, which were washed before analysis. After removal, the lungs were diced, passed through an 18-gauge needle, and digested in 5 ml RPMI medium containing 1 mg ml<sup>-1</sup> collagenase A and 200 µg DNase for 45 min at 37 °C. The lung homogenate was filtered through a 40 µm strainer, cells were washed, and red blood cells were lysed using lysis buffer (0.846% NH<sub>4</sub>Cl). These preparations were then used for flow cytometry, and the absence of CD45 and expression of CD102 and CD31 were used to identify ECs. For the data sets presented, cell populations were pre-gated on CD45<sup>-ve</sup>CD102<sup>+ve</sup> cells and, based on a comparison with the fluorescent minus one (FMO) control, almost 100% of these cells were CD31<sup>+ve</sup>. To identify infected ECs, the data shown were pre-gated on CD45<sup>-ve</sup>CD102<sup>+ve</sup> cells and were presented showing CD31 expression versus tdTomato. A similar procedure was performed for the isolation of brain mononuclear cells, but the cell suspension was fractionated on a 30–60% percoll gradient.

**Flow-cytometric analysis and Amnis ImageStream.** Freshly isolated ECs were stained in FACS buffer (0.5% BSA, 2 mM EDTA in PBS). Cells were stained with CD45-APC-eFluor-780 antibodies purchased from eBioscience and with CD31 (PECAM1)-AF488 and CD102(ICAM2)-AF647 purchased from Biolegend. The stained samples were run on an LSRFortessa cell analyser, and the results were analysed using FlowJo software (TreeStar). Whole blood was obtained by cardiac puncture. To prevent coagulation, whole blood was collected in 3.8% sodium citrate. For the detection of free parasites, whole blood was diluted in PBS and immediately subjected to analysis on the LSRFortessa cell analyser. Free parasites were identified by their size and expression of tdTomato. The gate for free parasite was drawn on freshly isolated tachyzoites from cell culture. Amnis ImageStream was used to visualize infected cells in the blood. White blood cells were purified using whole blood from infected mice, which was layered on top of Lympholyte (Cedarlane) and centrifuged at room temperature. The mononuclear preparation was removed and washed in FACS buffer. Cells were then stained in FACS buffer with CD11b-APC-eFluor-780, CD11c-APC and Gr1-PE-Cy7 from eBioscience and CD3-FITC from BD Biosciences. The stained samples were then used for analysis.

**Adoptive transfer of infected monocytes.** Monocytes were isolated from femur and tibia of naive mice using a monocyte isolation kit (#130-100-629, Miltenyi Biotec). Isolated monocytes were stained with CellTrace Violet (Life Technologies) in PBS at 37 °C. After staining, cells were washed twice with RPMI medium containing 10% FBS. Monocytes were then infected for 1 h with CPS-Cre-mCherry with a multiplicity of infection (MOI) of 1/20 in media containing 10% FBS at 37 °C. After infection, cells were washed twice with PBS and 1 × 10<sup>6</sup> cells were i.v. transferred into naive or previously infected mice. To distinguish cell populations localized in the vascular or extravascular compartments, mice were injected i.v. with CD45-APC-eFluor-780. Within 10 min, the mice were euthanized, and mononuclear cells from the brain were prepared as described above and assessed by flow cytometry.

**Fluidic experiments.** Microfluidic devices were fabricated using polydimethylsiloxane and coverglass, coated with fibronectin, and seeded with human umbilical vein endothelial cells (HUVECs, Lonza), as described previously<sup>42</sup>. In the Lodoen laboratory, mycoplasma screening was performed in all parasite and cell culture lines, monthly and whenever they obtained or thawed new lines. All cells used in these studies were mycoplasma negative. HUVECs were cultured for at least 24 h to a confluent monolayer before experimentation. The barrier integrity of the HUVECs was assayed by trans-epithelial electric resistance (TEER) assays and fluorescein isothiocyanate (FITC)-dextran transwell assays. Fluidic channels were perfused with 2.88 × 10<sup>8</sup> GFP expressing type II PA7 tachyzoites at shear forces of 1, 3, 6 or 10 dyn cm<sup>-2</sup> using an 11 Plus dual syringe pump (Harvard Apparatus), as described previously<sup>42,43</sup>. Parasites were flowed for 1 h, after which the monolayer was immediately fixed with 4% paraformaldehyde. To quantify parasite invasion, the monolayer was permeabilized and stained for vacuolar GRA7<sup>44</sup>. Anti-GRA7 antibody (12B6) was a gift from P. Bradley (University of California). Fluorescence and differential interference contrast images were acquired on a Nikon Eclipse TI inverted fluorescence microscope using ×20 and ×40 objectives. ImageJ was used to quantify intracellular parasites per 100 HUVECs from at least 22 fields of view for each independent experiment. Non-blinded experiments were performed using technical duplicates or triplicates for the fluidic channels, and for each condition there were two or three biological replicates.

Received 21 September 2015; accepted 23 December 2015;  
published 15 February 2016

## References

- Montoya, J. G. & Liesenfeld, O. Toxoplasmosis. *Lancet* **363**, 1965–1976 (2004).
- Kristensson, K. Microbes' roadmap to neurons. *Nature Rev. Neurosci.* **12**, 345–357 (2011).
- Kim, K. S. Mechanisms of microbial traversal of the blood–brain barrier. *Nature Rev. Microbiol.* **6**, 625–634 (2008).
- Lambert, H. & Barragan, A. Modelling parasite dissemination: host cell subversion and immune evasion by *Toxoplasma gondii*. *Cell. Microbiol.* **12**, 292–300 (2010).
- Iannaccone, M. *et al.* Subcapsular sinus macrophages prevent CNS invasion on peripheral infection with a neurotropic virus. *Nature* **465**, 1079–1083 (2010).
- Courtet, N. *et al.* CD11c- and CD11b-expressing mouse leukocytes transport single *Toxoplasma gondii* tachyzoites to the brain. *Blood* **107**, 309–316 (2006).
- Coureuil, M. *et al.* Meningococcal type IV pili recruit the polarity complex to cross the brain endothelium. *Science* **325**, 83–87 (2009).
- Barragan, A. Transepithelial migration of *Toxoplasma gondii* is linked to parasite motility and virulence. *J. Exp. Med.* **195**, 1625–1633 (2002).
- Ring, A., Weiser, J. N. & Tuomanen, E. I. Pneumococcal trafficking across the blood–brain barrier. Molecular analysis of a novel bidirectional pathway. *J. Clin. Invest.* **102**, 347–360 (1998).
- Shi, M. *et al.* Real-time imaging of trapping and urease-dependent transmigration of *Cryptococcus neoformans* in mouse brain. *J. Clin. Invest.* **120**, 1683–1693 (2010).
- Coombes, J. L. *et al.* Motile invaded neutrophils in the small intestine of *Toxoplasma gondii*-infected mice reveal a potential mechanism for parasite spread. *Proc. Natl Acad. Sci. USA* **110**, E1913–E1922 (2013).
- Chantanav, T. *et al.* Dynamics of T cell, antigen-presenting cell, and pathogen interactions during recall responses in the lymph node. *Immunity* **31**, 342–355 (2009).
- Drevets, D. A. *et al.* The Ly-6Chigh monocyte subpopulation transports listeria monocytogenes into the brain during systemic infection of mice. *J. Immunol.* **172**, 4418–4424 (2004).
- Coombes, J. L. & Robey, E. A. Dynamic imaging of host-pathogen interactions *in vivo*. *Nature Rev. Immunol.* **10**, 353–364 (2010).
- McGavern, D. B. & Kang, S. S. Illuminating viral infections in the nervous system. *Nature Rev. Immunol.* **11**, 318–329 (2011).
- Harris, T. H. *et al.* Generalized Lévy walks and the role of chemokines in migration of effector CD8<sup>+</sup> T cells. *Nature* **486**, 545–548 (2012).
- Xu, H.-T., Pan, F., Yang, G. & Gan, W.-B. Choice of cranial window type for *in vivo* imaging affects dendritic spine turnover in the cortex. *Nature Neurosci.* **10**, 549–551 (2007).
- Garlanda, C. & Dejana, E. Heterogeneity of endothelial cells: specific markers. *Arterioscler. Thromb. Vasc. Biol.* **17**, 1193–1202 (1997).
- Williams, R. W. Mapping genes that modulate mouse brain development: a quantitative genetic approach. *Results Probl. Cell Differ.* **30**, 21–49 (2000).
- Fox, B. A. & Bzik, D. J. *De novo* pyrimidine biosynthesis is required for virulence of *Toxoplasma gondii*. *Nature* **415**, 926–929 (2002).
- Dupont, C. D. *et al.* Parasite fate and involvement of infected cells in the induction of CD4+ and CD8+ T cell responses to toxoplasma gondii. *PLoS Pathog.* **10**, e1004047 (2014).
- Lambert, H., Vutova, P. P., Adams, W. C., Lore, K. & Barragan, A. The *Toxoplasma gondii*-shuttling function of dendritic cells is linked to the parasite genotype. *Infect. Immun.* **77**, 1679–1688 (2009).
- Glatman Zaretsky, A. *et al.* Infection with *Toxoplasma gondii* alters lymphotoxin expression associated with changes in splenic architecture. *Infect. Immun.* **80**, 3602–3610 (2012).
- Papaioannou, T. G. & Stefanadis, C. Vascular wall shear stress: basic principles and methods. *Hellenic J. Cardiol.* **46**, 9–15 (2005).
- Bernard, S. C. *et al.* Pathogenic *Neisseria meningitidis* utilizes CD147 for vascular colonization. *Nature Med.* **20**, 725–731 (2014).
- Lefort, C. T. *et al.* Distinct roles for talin-1 and kindlin-3 in LFA-1 extension and affinity regulation. *Blood* **119**, 4275–4282 (2012).
- Mairey, E. *et al.* Cerebral microcirculation shear stress levels determine *Neisseria meningitidis* attachment sites along the blood–brain barrier. *J. Exp. Med.* **203**, 1939–1950 (2006).
- Lee, W.-Y. *et al.* An intravascular immune response to *Borrelia burgdorferi* involves Kupffer cells and iNKT cells. *Nature Immunol.* **11**, 295–302 (2010).
- Lee, W. Y. *et al.* Invariant natural killer T cells act as an extravascular cytotoxic barrier for joint-invading Lyme Borrelia. *Proc. Natl Acad. Sci. USA* **111**, 13936–13941 (2014).
- Liu, T.-B. *et al.* Brain inositol is a novel stimulator for promoting cryptococcus penetration of the blood–brain barrier. *PLoS Pathog.* **9**, e1003247 (2013).
- Matsuda, K. *et al.* Characterization of simian immunodeficiency virus (SIV) that induces SIV encephalitis in rhesus macaques with high frequency: role of TRIM5 and major histocompatibility complex genotypes and early entry to the brain. *J. Virol.* **88**, 13201–13211 (2014).
- Koshy, A. A. *et al.* Toxoplasma co-opts host cells it does not invade. *PLoS Pathog.* **8**, e1002825 (2012).

33. Ma, J. S. *et al.* Selective and strain-specific NFAT4 activation by the *Toxoplasma gondii* polymorphic dense granule protein GRA6. *J. Exp. Med.* **211**, 2013–2032 (2014).
34. Lambert, H., Hitziger, N., Dellacasa, I., Svensson, M. & Barragan, A. Induction of dendritic cell migration upon *Toxoplasma gondii* infection potentiates parasite dissemination. *Cell. Microbiol.* **8**, 1611–1623 (2006).
35. Germain, R. N., Robey, E. A. & Cahalan, M. D. A decade of imaging cellular motility and interaction dynamics in the immune system. *Science* **336**, 1676–1681 (2012).
36. Maisner, A., Neufeld, J. & Weingartl, H. Organ- and endotheliotropism of Nipah virus infections *in vivo* and *in vitro*. *Thromb. Haemost.* **102**, 1014–1023 (2009).
37. Su, C. Recent expansion of toxoplasma through enhanced oral transmission. *Science* **299**, 414–416 (2003).
38. Turner, L. *et al.* Severe malaria is associated with parasite binding to endothelial protein C receptor. *Nature* **498**, 502–505 (2013).
39. Wille, U. *et al.* IL-10 is not required to prevent immune hyperactivity during memory responses to *Toxoplasma gondii*. *Parasite Immunol.* **26**, 229–236 (2004).
40. Koshy, A. A. *et al.* Toxoplasma secreting Cre recombinase for analysis of host-parasite interactions. *Nature Methods* **7**, 307–309 (2010).
41. Yang, G., Pan, F., Parkhurst, C. N., Grutzendler, J. & Gan, W.-B. Thinned-skull cranial window technique for long-term imaging of the cortex in live mice. *Nature Protoc.* **5**, 201–208 (2010).
42. Harker, K. S., Jivan, E., McWhorter, F. Y., Liu, W. F. & Lodoen, M. B. Shear forces enhance *Toxoplasma gondii* tachyzoite motility on vascular endothelium. *mBio* **5**, e01111 (2014).
43. Harker, K. S. *et al.* *Toxoplasma gondii* modulates the dynamics of human monocyte adhesion to vascular endothelium under fluidic shear stress. *J. Leukocyte Biol.* **93**, 789–800 (2013).
44. Dunn, J. D., Ravindran, S., Kim, S. K. & Boothroyd, J. C. The *Toxoplasma gondii* dense granule protein GRA7 is phosphorylated upon invasion and forms an unexpected association with the rhoptry proteins ROP2 and ROP4. *Infect. Immun.* **76**, 5853–5861 (2008).

## Acknowledgements

C.K. was supported by research grant KO 4609-1/1 from the German Research Foundation (DFG). This work was supported by grants from the National Institutes of Health (NIH AI 41158 to C.A.H., NIH NS065116 to A.A.K., NIH AI041930 to D.J.B.), the American Heart Association (14BGIA20380675 to M.B.L. and 15POST25550021 to N.U.) and the University of Arizona and the BIO5 Institute (A.A.K.). Imaging experiments were performed in the PennVet Imaging Core Facility on instrumentation supported by NIH S10RR027128, the School of Veterinary Medicine, the University of Pennsylvania, and the Commonwealth of Pennsylvania. sIgM-ko mice were provided by G. Debes (University of Pennsylvania). C.A.H is the Mindy Halikman Heyer President's Distinguished Chair.

## Author contributions

C.K. performed the majority of the experiments. N.U. and M.B.L. performed and analysed the microfluidic chamber experiments. J.D. and G.H.P. helped with sample collection. D.J.B. provided the CPS parasites. A.A.K. provided Cre-secreting parasites. D.A.C., J.H. and D.B.M were involved in study design. C.K. and C.A.H. wrote the paper. All authors discussed the results and commented on the manuscript.

## Additional information

Supplementary information is available online. Reprints and permissions information is available online at [www.nature.com/reprints](http://www.nature.com/reprints). Correspondence and requests for materials should be addressed to C.A.H.

## Competing interests

The authors declare no competing financial interests.